Coupling of Hydrologic Effects to Borehole Strain Data

Evelyn Roeloffs, USGS
July 2005

1. Introduction

The entire period range over which borehole strainmeters are useful can be subdivided into several smaller ranges.

High-frequency data (100 or 200 sps) from some dilatometers and from the mini-PBO Sakata-type 3-component strainmeters has been recorded and appears to be of good quality. However, few quantitative comparisons have been made between these data and seismic recordings. Little or no data has been available from the GTSM's at sampling intervals shorter than 5 minutes. 20-sps data from new PBO installations will allow the performance of these instruments to be investigated in the high-frequency range.

The tidal band was discussed above. It is unusual for a borehole strainmeter to fail to record any tides. For most dilatometers, agreement between observed and reference areal strain phases is very good. The situation is not quite so simple for GTSM shear strains.

However, it is for periods longer than about 10 days that the most challenging questions arise as to the meaningfulness of borehole strainmeter data. At these periods, other factors can affect the data, many of which are hydrologic.

Topics covered in this section:
1) Response to rainfall and snow loading
2) Basic poroelastic coupling and fluid flow
3) Direct effects of fluid pressure changes on the strainmeter
4) Hydrologic influences on post-earthquake strain changes.
5) Drainage effects

2. Snow and Rainfall Loading

Borehole strainmeters are sensitive enough to detect the weight of rain or snow on the earth's surface. Shallow tiltmeter installations and creepmeters are notoriously affected by rainfall, often exhibiting large excursions that continue after the rainfall has stopped, and which are attributable to nonlinear behavior of soft, weathered, near-surface materials. It is important to understand the the responses to rainfall recorded by borehole strainmeters installed in rock of low porosity, at depths of 100 meters or more, are of an entirely different origin and reflect the instrument's very high sensitivity.

Figure 1 illustrates the setting of the Devil's Postpile dilatometer at Long Valley caldera, California. The geology consists of basalt flows with permeable tops, overlying older, lower porosity granite bedrock. During drilling of the strainmeter borehole, a productive aquifer was encountered at a depth of 43 m; the strainmeter is installed well below this aquifer in the granite. The observation well was added later to monitor fluid pressure in the aquifer.

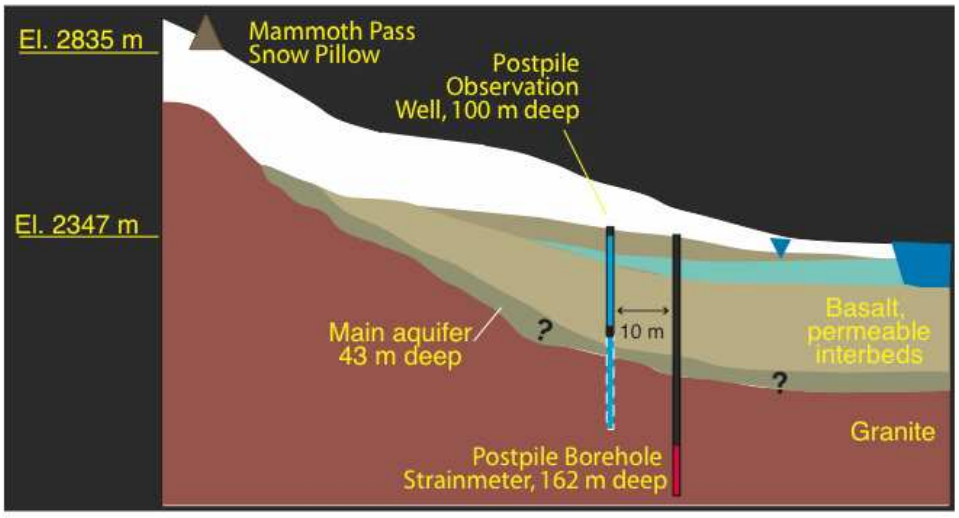

Figure 1. Cartoon showing setting of the Devil's Postpile dilatometer, Long Valley, California

The Mammoth Pass snow pillow provides a source of snow data near the strainmeter; the data are the weight of the snow on the pillow and so are a direct measure of the applied surface load. (The data from this snow pillow and others can be accessed at the CDEC website; see Online Resources at the end of these notes). Snow lands on the ground and stays there, rather than infiltrating or running off, and therefore provides a simpler load than rainfall. Figure 2 shows the snow water content data from Mammoth Pass.

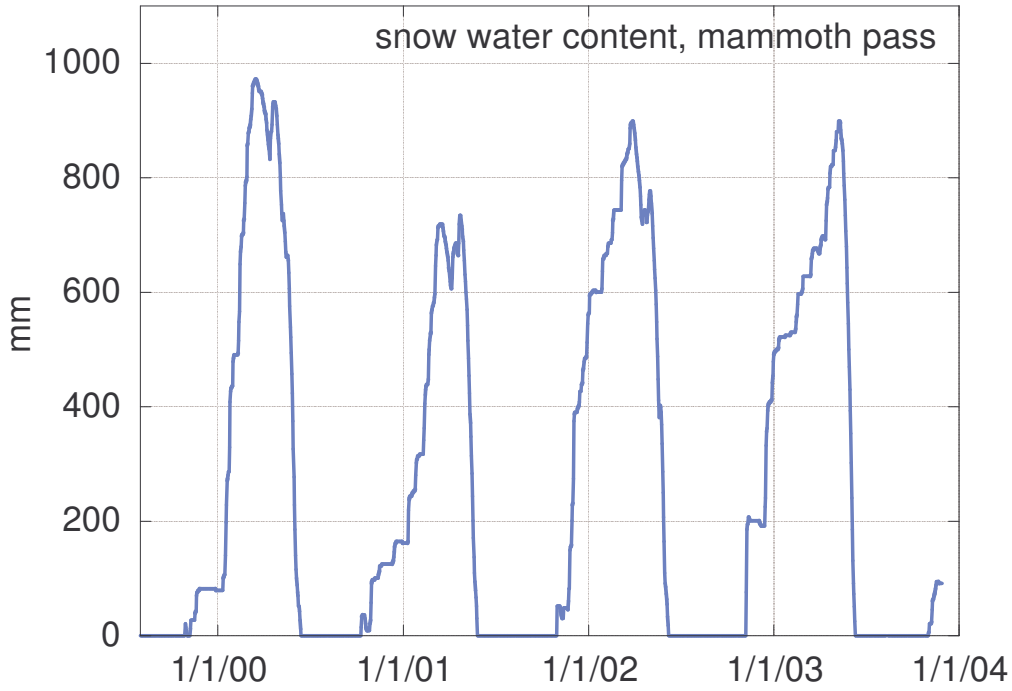

Figure 2. Snow water content at Mammoth Pass, California (from CDEC web site)

Linear regression of the strain data against atmospheric pressure shows that an atmospheric pressure increase produces a contractional strain change of 2.9 to 3.7 nanostrain/millibar, which is a measure of the surface-loading efficiency. Multiplying this times the snow load gives the result shown in Figure 3.

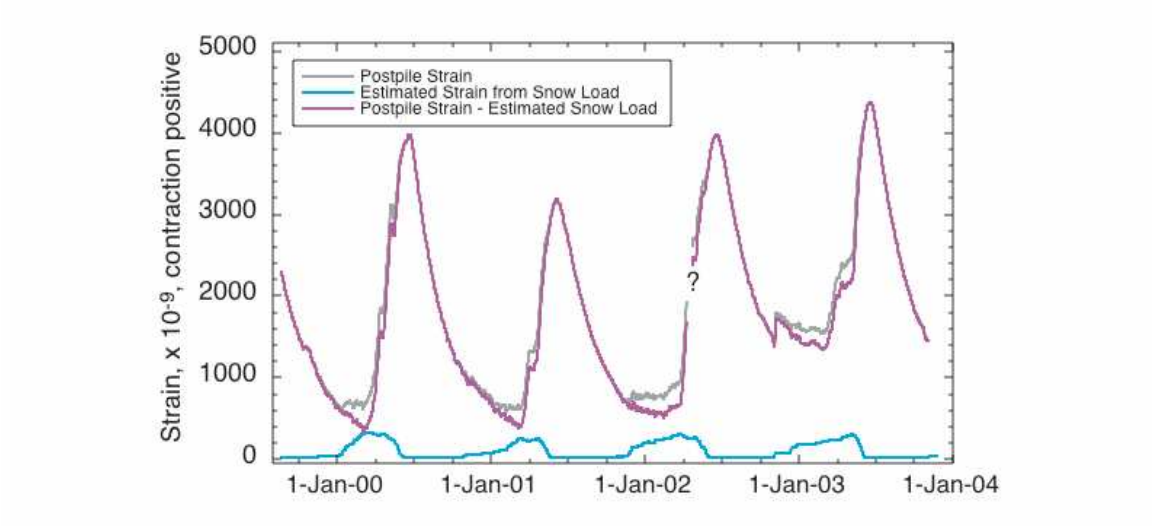

Figure 3. Snow load component of Postpile strain

At Postpile, the snow load is a small but distinct influence on the strainmeter data. Because the snow is a static load, it can be corrected for by just removing a scaled version of the snow water content data. Obviously snow loading is not a large part of the seasonal cycle at Postpile; we will return to this later.

Like snow, rainfall applies a surface load. However, it does not stay on the ground above the strainmeter, or accumulate there. So generally rainfall loading steps are smaller than snow loading steps, and they dissipate over a period of days. If rainfall loading steps occur, then they usually occur during low values of atmospheric pressure. Therefore,when determining the strainmeter's response to atmospheric pressure, it may be necessary to select a stretch of data without rainfall.

Should rainfall loading show up on GTSM data? Surface loads do produce horizontal strain, so in principle, rainfall loading can be observed in time series of individual gauge components, or in areal strain components. Rainfall is not expected to produce significant shear strain, but should always be evaluated as a possible contributor to borehole strainmeter signals.

3. Coupling of fluid pressure and strain

Subsurface fluid pressure and strain are coupled. The reason is that deforming a rock changes the volume of pore space. Unless fluid can escape or enter the deformed

volume (as it can near the water table), the pore volume change causes the pore fluid pressure to change. Conversely, fluid-pressure changes in subsurface rocks deform the rock. Non-uniform fluid pressures generally dissipate with time due to fluid flow, and therefore the coupled strains are also time-varying.

3.1 Measuring Subsurface Fluid Pressure

Subsurface fluid pressure fluctuations can be measured directly in a borehole sealed from the atmosphere, or groundwater level can be measured in an open well, which acts as a manometer. The variation in groundwater level, Δh, is related to the pressure variation, Δp, as $\Delta p = \rho g \Delta h$, where g is the acceleration due to gravity and ρ is the density of fluid. Groundwater level is essentially a direct measurement of formation fluid pressure, except at "high" frequencies, where a measurement in an open well will not track formation pressure. The definition of "high frequency" depends on the hydraulic diffusivity of the formation.

It is now recognized that subsurface fluid pressure variations influence borehole strainmeter data, and PBO strainmeter boreholes will all include pore pressure monitors. For existing California borehole strainmeters, fluid pressure data are available from nearby wells, but only in a few cases from the same borehole.

3.2 "Undrained" Pore Pressure-Strain Coupling

The term "undrained" refers to a an ideal situation where a volume of subsurface rock is deformed, but no fluid flow occurs. Real-world situations where undrained conditions are approximated include: the instant after an earthquake has taken place, and tidal deformation in formations isolated from the water table (wavelengths are long so spatial gradients are too small to induce significant flow). Undrained conditions are also assumed to apply as an initial condition when a stress or strain is applied abruptly at time zero.

The ratio of fluid pressure change to strain under undrained conditions depends critically on certain properties of the formation. For many rocks in which void space is distributed approximately uniformly in the form of pores, changes of pore volume occur primarily with rock deformation that changes the overall volume of the rock. That is,

shear deformation with no associated volume change is not strongly coupled to fluid pressure. For a rock in which void space is dominated by fractures with a preferred orientation, fluid pressure in the fractures is most strongly coupled to deformation that is normal to the plane of the fractures.

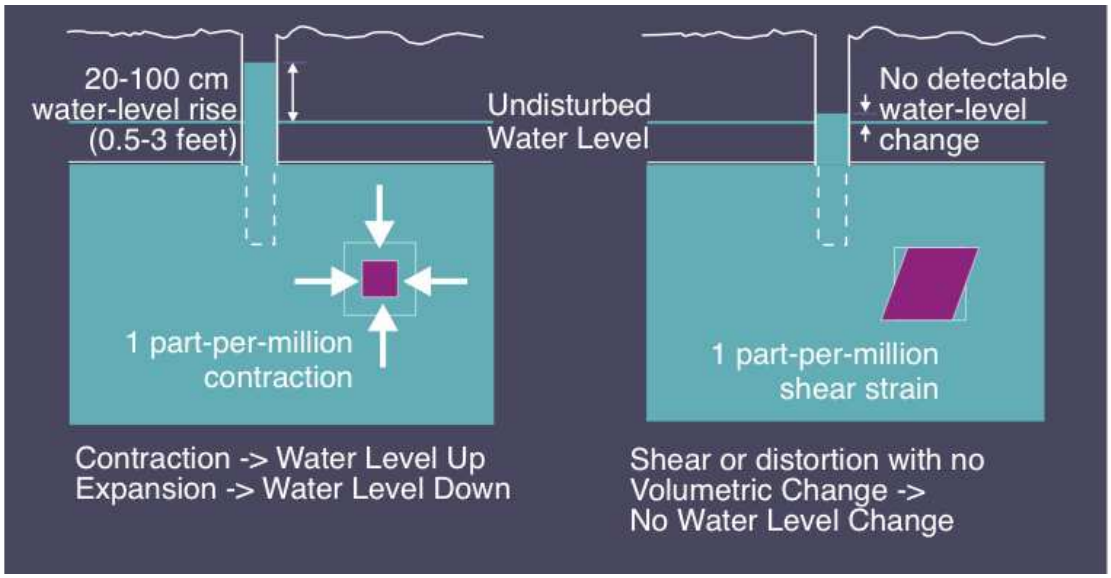

Figure 4. Cartoon illustrating different fluid pressure response to shear strain vs. volumetric strain.

The mathematical formulation for the coupling between the elastic deformation of a porous rock and the pressure of fluids in the pores was first developed by Biot (1956, 1941). Wang (2000) provides an updated comprehensive summary. Of chief importance to understanding water-level fluctuations coupled to crustal deformation is that, in the absence of fluid flow (undrained conditions), fluid-pressure changes are proportional to changes in average stress, $\Delta\sigma_{kk}$ or, equivalently, in volumetric strain, $\Delta\varepsilon_{kk}$, according to

$$\Delta p = -B\Delta\sigma_{kk} = -(BK_u)\Delta\varepsilon_{kk}. \qquad (1)$$

In equation (1), the minus signs are needed because pore pressure decreases with positive (extensional) stress or strain. B, known as Skempton's coefficient, is a dimensionless material property with a value between 0 and 1, and K_u is the porous material's undrained bulk modulus. There are few measurements of Skempton's coefficient from laboratory work, but those that exist confirm this range of values. Moreover, Skempton's coefficient and the undrained bulk modulus can also be inferred from other rock properties: rock bulk modulus, porosity, fluid and grain compressibility. These

calculations, observations of Earth tides in wells, and laboratory studies suggest that the coefficient of proportionality between water-level changes and volumetric strain is in the range of 30-100 cm/microstrain for rocks whose void space is in the form of pores. In a homogeneous, isotropic rock no coupling is expected between shear strain and fluid pressure.

In a rock where void space is dominated by fractures, the sensitivity of water pressure to strain can be greater than in a porous rock, but is not as easily calculated based on rock properties because the coefficient depends on fracture compliance. Bower (1983) has shown how to relate fracture parameters to observed Earth tide response. Observed coefficients of water-level change in response to strain in fracture-dominated formations are as high as 2 m/microstrain (*e.g.*, Woodcock and Roeloffs, 1996). Because such formations are anisotropic, regional shear strain can in principle be coupled to local fluid pressure variations.

If undrained conditions truly exist, then the fluid-saturated rock mass can simply be thought of as an elastic material whose shear modulus is the same as that of the rock itself, but with an "undrained" Poisson ratio, ν_u, such that $\nu < \nu_u < 0.5$. There is no fluid flow and no induced time-dependent strain.

3.3 Strain-fluid pressure coupling when conditions are not undrained

Subsurface fluid pressure varies in response to rainfall, pumping, or any other factor changing the mass of fluid in the system. When fluid mass per unit volume of material is not constant, equation (1) generalizes to

$$\Delta p = BK_u \left[-\Delta\varepsilon_{kk} + \frac{1}{1 - K/K_s} \frac{m - m_0}{\rho_0} \right] \qquad (2)$$

where K is the (drained) bulk modulus of the material, K_s is the bulk modulus of the solid grains, and $(m - m_0)/\rho_0$ is the change in fluid mass per unit volume, divided by the fluid density in a reference state. Equation (2) shows that fluid-mass changes are coupled not only to fluid pressure changes, but also to volumetric strain changes.

3.4 Strainmeter signals produced by pore fluid pressure acting on the strainmeter

Segall et al. (2003) pointed out that increasing fluid pressure would apply compressional stress to borehole strainmeters and produce contractional signals that do not represent strain of the rock. Under isotropic conditions, the fluid pressure changes would be expected to affect only areal or volumetric strain, not the shear strain. From equation (14) of Segall et al. (2003), the ratio u_p / u_ε of instrument output in response to fluid pressure change, to instrument output in response to volumetric strain of the rock, is

$$u_p / u_\varepsilon = \frac{3(\nu_u - \nu)(1+\alpha)}{2GB(1+\nu_u)} \qquad (3)$$

where ν is the drained Poisson ratio, ν_u is the undrained Poisson ratio, B is Skempton's coefficient, and G is the shear modulus (all for the rock in which the strainmeter is installed), and α is the ratio of strainmeter output for a change in vertical strain to strainmeter output for a change in radial strain. Note that α is not really known, but is probably much smaller than 1 for a GTSM. An important fact about equation (3) is that it predicts an apparent contractional strain signal in response to increasing fluid pressure. This differs from the response of the crust itself in the absence of a strainmeter, for which poroelastic coupling predicts extensional strain when fluid pressure rises. The reason is that the strainmeter is an essentially impermeable inclusion. Table 1 lists some computed values of u_p / u_ε for plausible values of ν , ν_u, B, G, and α.

Table 1. Ratio of strainmeter output in response to fluid pressure change, to output in response to volumetric strain change. Calculated from Segall et al. (2003) equation (13)

Drained Poisson Ratio ν	Undrained Poisson Ratio ν_u	Skempton's coefficient B	α	Shear modulus, G (GPa)	u_p / u_ε, per m H2O / per microstrain
0.25	0.35	1.00	1	33	0.067
0.25	0.35	0.50	1	33	0.135
0.25	0.30	1.00	1	33	0.035

0.25	0.30	1.00	0	33	0.017
0.25	0.35	1.00	1	10	0.222
0.20	0.35	1.00	1	10	0.333
0.20	0.35	1.00	1	3	1.111

3.5 Seasonal Strain Signals at the Long Valley Postpile Dilatometer

We return to the Postpile dilatometer data shown in Figure 3, which show that there is a seasonal strain signal with an amplitude of 2 to 3.5 microstrain, of which only a small part is attributable to snow loading. Figure 5 shows the strain data after the (small) snow load correction and the fluid pressure data from the nearby borehole.

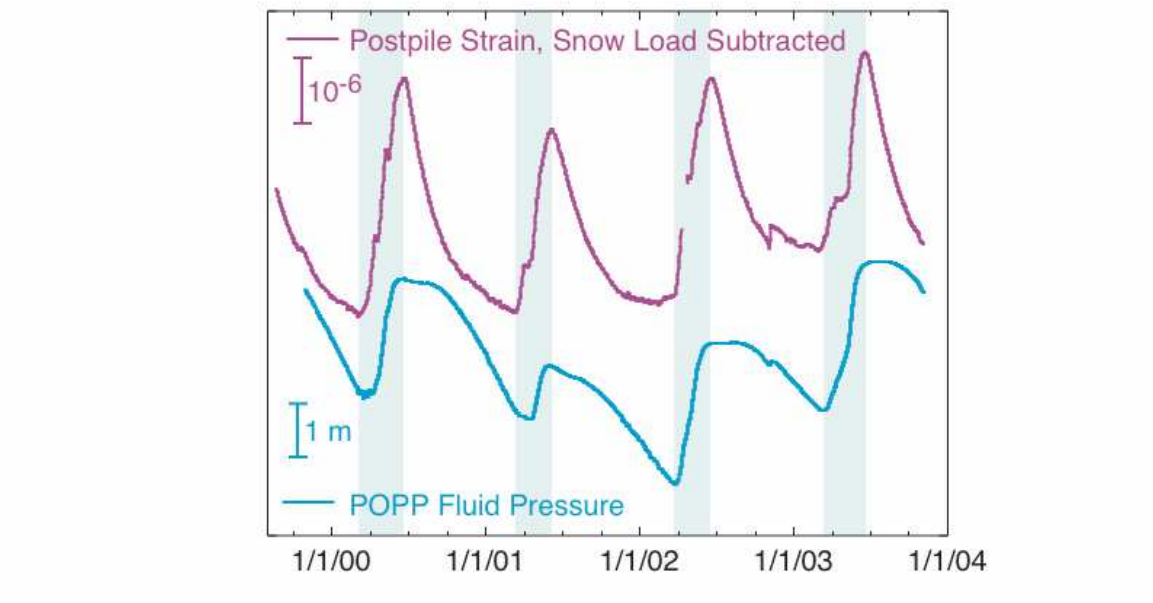

Figure 5. Postpile dilatometer data, corrected for snow loading, together with fluid pressure data from a borehole 10 m away.

Fluid pressure is measured in a separate borehole about 10 m from the strainmeter. The fluid pressure borehole is cased to just above the "main aquifer", which is at the base of a permeable basalt flow. The fluid pressure borehole is left open to depths in the underlying granite comparable to the depth of the strainmeter. The fluid pressure

measured with this configuration will be an average of the pressures in the permeable aquifer and the granite.

In Figure 5, the periods of seasonal contractional strain are highlighted to show that they correspond closely with the times when fluid pressure is increasing (which coincide almost exactly with the times when snow is melting). Although the times of peaks and troughs correspond, the actual time histories of fluid pressure and strain change are somewhat different. However, comparing the net annual changes in strain and in water level yields a ratio of strain change to fluid pressure change between 1 and 3 microstrain/m of water level change. The observed effect of the fluid pressure on the strain data is consistent with the principle proposed by Segall et al. (2003), in that the contractional strain coincides with increasing fluid pressure, consistent with the effect being due to the pressure of the fluid acting on the relatively impermeable strainmeter/grout inclusion. However, the ratio of observed strain to fluid pressure change is at the high end of the values expected. A value as high as 1 microstrain/m of water is obtained only for a low shear modulus (3 GPa) and a large difference between ν and ν_u (0.25 and 0.35, respectively).

Although the seasonal strain changes at the Postpile site are qualitatively consistent with what's expected from fluid pressure acting on the strainmeter, the fluid pressure data at the Postpile site cannot be used with just a simple technique like linear regression to correct the seasonal signal in the strain data. One possibility is that the fluid pressure measurement made in a separate borehole, which is open not only to the granite in which the strainmeter is installed, but also to a much more permeable formation, does not track the fluid pressure in the immediate vicinity of the strainmeter. It is also possible that the strainmeter experiences some degree of strain from deformation of the overlying active aquifer as the pressure in that aquifer changes.

3.6 Seasonal Signals at Parkfield Donna Lee Site

Figure 6 shows data from the Parkfield Donalee GTSM, Donalee dilatometer, and Joaquin Canyon water well. The GTSM data are the areal and shear strains prepared by CSIRO, which have been detrended by subtracting a combination of exponential

functions, allowing some variations with periods of a few years to remain. The dilatometer data have been detrended by subtracting a curve fit to 6-month averages, which will suppress such variations. The water level data have not been detrended.

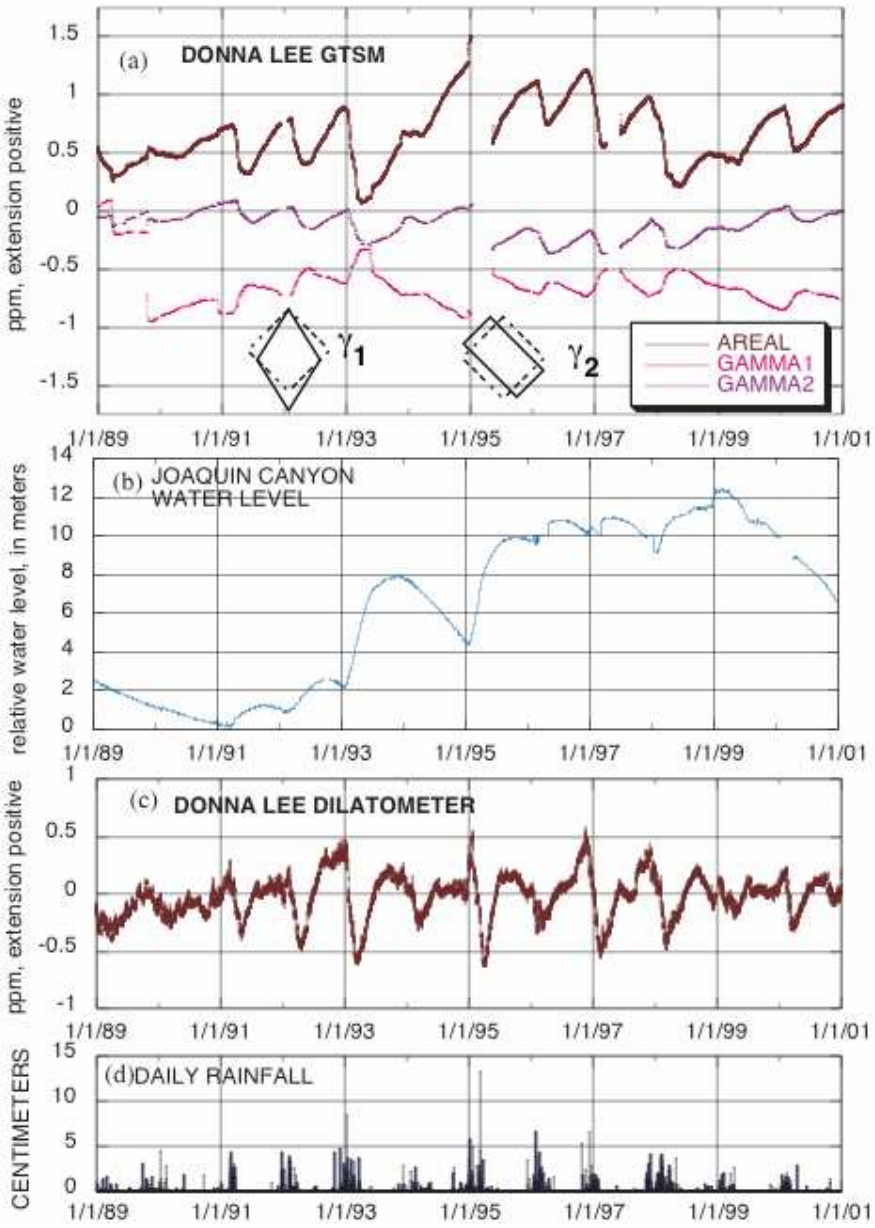

Figure 6. Data from the Parkfield Donna Lee site. Details in text.

The Joaquin Canyon water well is located about 500 m from the strainmeter boreholes, which are less than 100 m apart. During drilling of the strainmeter boreholes, an aquifer was encountered that produced large quantities of water. The water well was

drilled through interbedded sand and clay, with a confining unit overlying a productive aquifer about 152 m below the surface. The water well is open to the formation from 147-153 m below the surface, so its water level is proportional to the pressure in this aquifer. The dilatometer is at a depth of 176.5 m and the GTSM is at a depth of 174 m; both are installed in sandstone. Although the depth at which the aquifer was encountered in the strainmeter boreholes is not known, it is probably the same formation as that monitored by the water well.

Variations with an approximately 1-year period are visible in all the strain data, including the shear strains. Contractional strain coincides closely with increasing fluid pressure for both the dilatometer and the GTSM areal strain, and maxima and minima of γ_2 and γ_1, respectively, coincide with peak extension. However, the amplitudes of the seasonal cycles in the water level data vary much more than the amplitudes of the seasonal strain cycles. The shear strain cycles approximately mirror each other and their time histories closely resemble the time history of areal strain recorded by the GTSM. The shapes of the annual cycles are distinctly different for the GTSM, water level, and dilatometer. The areal and volumetric strain vary of the order of 0.5 microstrain/m of water, comparable to the Postpile dilatometer, and at the high end of the range of coefficients relating fluid pressure to strainmeter output (Table 1).

The seasonal variations in shear strain are about half as large as those in areal strain, which is not expected in a model based on a uniform, isotropic porous elastic medium. The poroelastic properties of Berea sandstone have been found to be anisotropic (e.g., *Lockner* [2002]) in that properties measured in the direction perpendicular to bedding differ from those measured parallel to bedding. However, anisotropy with respect to the two bedding-parallel directions would seem to be required to induce shear strain via a change in the fluid pressure in the formation surrounding the strainmeter. Shear strain imposed by deformation of the aquifer itself seems a more likely explanation.

The differences between the shapes of the seasonal strain cycles and the water level cycles, the smaller year-to-year variability of the strain cycles, the large shear strains, and the relatively large coefficient between fluid pressure change and areal and vertical strain suggest that another mechanism may be operating. Temperature changes

induced by infiltration of precipitation are a candidate. The strainmeters are reputed to be be extremely temperature sensitive, but the exact coefficient relating strainmeter output to ambient temperature of the rock around the sensor is not known. Groundwater temperature changes of 0.001-0.01ºC due to influx of meteoric water seem feasible and should be evaluated as a contributing factor in seasonal strain variations.

4. Time-dependent drainage effects

Undrained fluid-pressure changes in response to strain occur instantaneously with deformation. In fact, the water-level variation would have the same time history as the deformation were it not for the ability of water to flow. Flow causes spatial variations in pressure to equilibrate with each other over a time scale governed by the material's hydraulic diffusivity. In particular, a sudden, localized change of pore pressure induced by a tectonic event such as an earthquake or rapid intrusion will spread and dissipate with time, causing time-dependent fluid pressure changes in locations not originally affected by the tectonic event.

4.1 Vertical flow to the water table

The vertical flow path between the subsurface and the water table (sometimes called "water table drainage") can have a huge effect on fluid pressures that are induced by strain, and, in principle, on data from borehole strainmeters. Here we will use operational definitions of "water table" and "confined" aquifers specific to the purposes of understanding their responses to strain. (We will also use the term "aquifer" for any subsurface saturated formation, whereas hydrologists usually reserve the term for formations that can supply useful quantities of water for human consumption.)

The water table is defined as the top of the zone of saturation. For our purposes, the important thing about the water table is that there is empty pore space above it (Fig. 7). If rock at the depth of the water table is deformed, fluid in the pores has the option of moving up or down into unoccupied pore space.

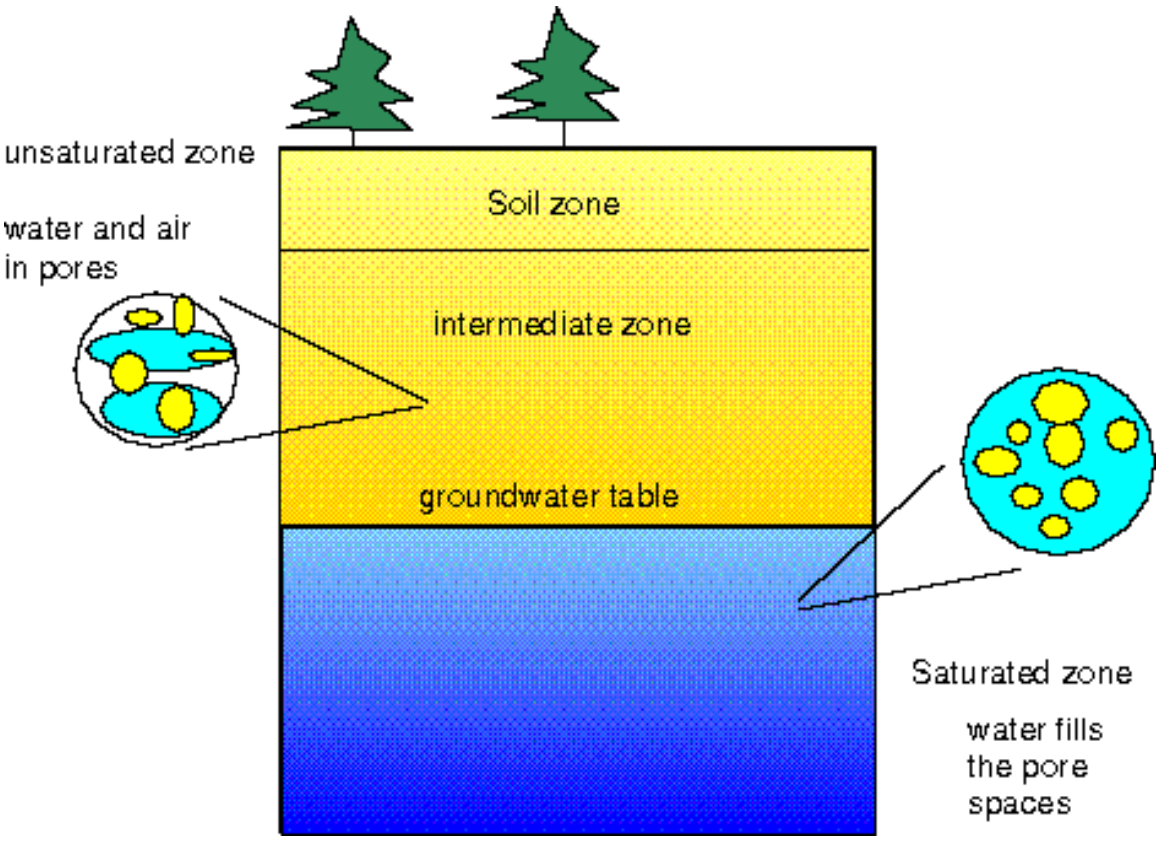

Figure 7. The water table. From topex.ucsd.edu/es10/ lectures/lecture22/ground.gif

A perfectly confined aquifer is the opposite of a water table aquifer - fluid in a confined aquifer, by definition, is not able to flow to the water table. Confinement can be created by a single highly impermeable layer, or by a significant thickness of moderately permeable material.

There is a very large difference between the amount by which the elevation of the water table must change, and the equivalent pressure head induced by a pressure change at depth. For example, a water-pressure rise of 0.01 MPa (1.45 psi) increases the water level in a well by 1 m. But the bulk modulus of water is 0.435 GPa^{-1}, so a fluid volume decrease of only 0.00044% can relieve the pressure increase, if fluid can escape from the system. In a 100-m thick aquifer with 10% porosity, removal of 0.000044 cubic meters from each 1-m square area of aquifer would relieve the pressure increase, while causing a barely-detectable water-table drop of only 0.44 mm. Thus, if strain is applied instantaneously, and remains in force, then the fluid pressure at depth will instantaneously change, while that at the water table will not. The water table can be

thought of as a constant-pressure boundary where no strain-induced fluid pressure changes can occur.

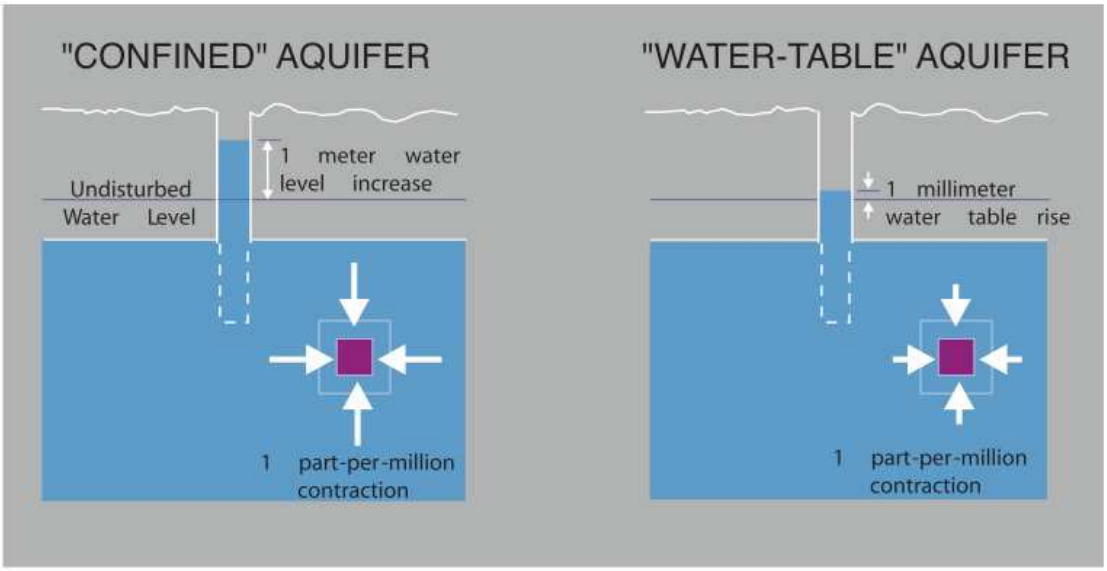

Figure 8. Difference in response to strain of a confined vs. a water-table aquifer.

Now consider what happens if a contractional tectonic strain of 1 microstrain is applied instantaneously, and is uniform over a depth large compared with that at which a strainmeter is installed. Coseismic strain is an example of this situation. At the depth of the strainmeter, the formation is better confined, and there will be an instantaneous fluid pressure increase of the order of 1 m. At the water table, however, there will be negligible pressure change. This pressure gradient will induce upward flow that will ultimately relieve the pressure at the depth of the strainmeter. The key question is, what is the time scale of this flow?

The material property that governs the time scale of transient fluid flow is the hydraulic diffusivity, c, which is related to other, more familiar, parameters of hydraulic conductivity by

$$c = k / S_s = T / S$$

where k is hydraulic conductivity (dimensions L/T), S_s is specific storage (dimensions 1/L), T is transmissivity (hydraulic conductivity times formation thickness) and S is the storage coefficient (product of specific storage and formation thickness). Typical values

of specific storage range from about 10^{-7}/m to 10^{-4}/m. Note that although T and c have the same dimensions, they have different physical meanings and their numerical values differ by many orders of magnitude. The hydraulic conductivity is related to permeability by:

(hydraulic conductivity)=

permeability*(fluid density)*(acceleration due to gravity)/(fluid viscosity)

Permeability is an intrinsic property of the rock; it has dimensions of L^2, and is usually expressed in darcies, with 1 darcy=10^{-12} m^2. 1 darcy corresponds to a hydraulic conductivity of approximately=10^{-5} m/s for water.

If the material between the depth, z , of the strainmeter and the depth, z_w, of the water table is assumed to have a uniform vertical hydraulic diffusivity, c, then the 1-D diffusion equation for groundwater flow can be solved analytically to yield the time history of pressure change, $p(z,t)$, caused by this vertical flow:

$$p(z,t) = -BK_u\varepsilon_0 erf\{[(z-z_w)^2/4ct]^{1/2}\} \quad (4)$$

In equation (4), erf denotes the error function and ε_0 denotes the amplitude of the instantaneously applied strain (Roeloffs, 1996). Equation (4) implies that the time required for strain-induced pressure to dissipate increases as the square of the depth below the water table, and decreases in inverse proportion to the hydraulic diffusivity. Since hydraulic diffusivity varies over many orders of magnitude (Figure 9), this time scale also varies tremendously (Figure 10).

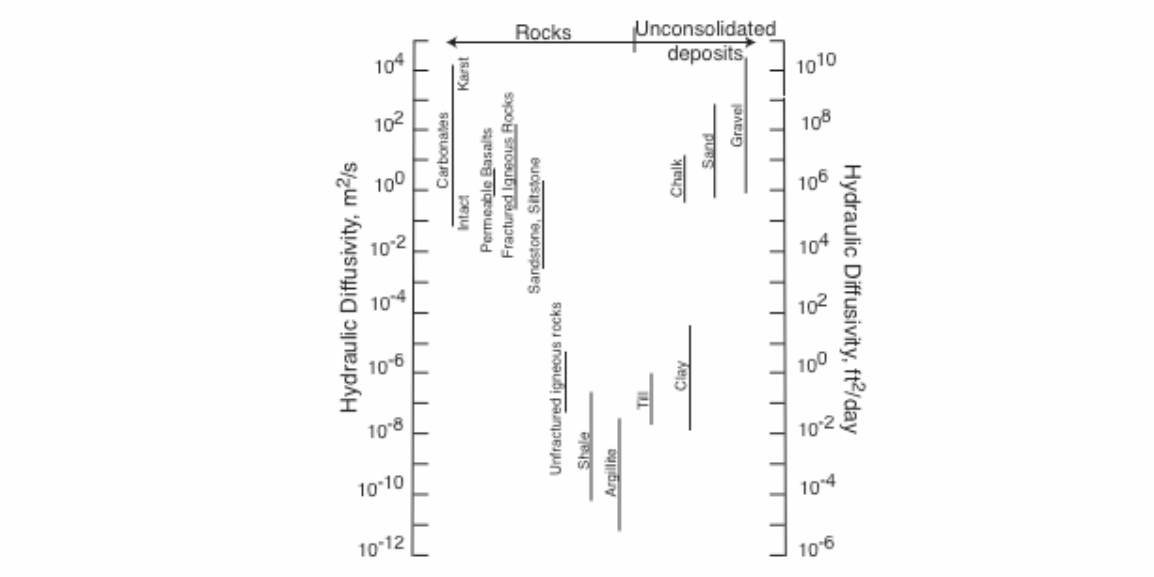

Figure 9. Approximate ranges of hydraulic diffusivity for various types of rock. From Roeloffs (1996).

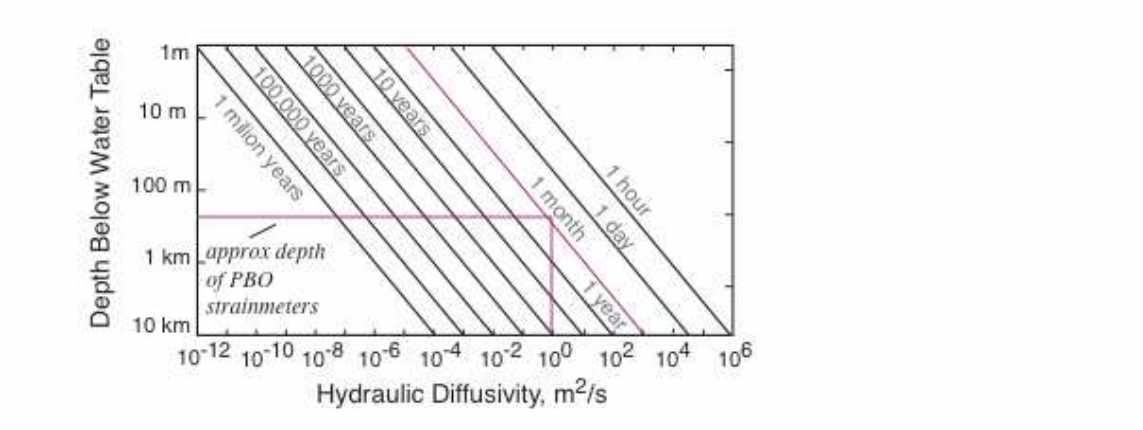

Figure 10. Approximate time for strain-induced transients to dissipate by flow to the water table. Each curve is given by $\omega(z-z_w)^2/c=0.2$, for ω corresponding to the indicated period. The graph gives the elapsed time after the imposition of a strain step such that the fluid pressure response has fallen to 0.1 times the undrained value. Equivalently, if oscillatory strain is imposed with the period indicated, the lines are combinations of depth and diffusivity such that drainage effects reduce the response by a factor of 1/*e*. From Roeloffs (1996).

Figure 10 shows the range of times over which strain-induced pressure would be expected to persist. This range of time scales is one basis for distinguishing "confined" from "unconfined" aquifers, for purposes of characterizing their responses to strain. The approximate depth of PBO strainmeters (200 m) is shown in pink. To avoid the drainage effects discussed below, it is desirable that this time be in excess of 1 month, implying that material with a vertical hydraulic diffusivity lower than 1 m^2/s should be chosen. Comparing this requirement with Figure 9 shows one reason why it is important to avoid material containing fractures when selecting a strainmeter site. Aquifer pumping or slug tests (e.g., Moench, 1985) can be used to determine the hydrologic properties of monitoring wells, and in some cases pumping tests can provide information on the connection between the monitored formation and the water table. Slug tests are being carried out on most of at least the initial PBO strainmeter boreholes.

4.2 Drainage effects on coseismic strain changes

When tectonic strain induces fluid pressure changes (e.g., fluid pressure increases in regions subjected to coseismic static contractional strain), these fluid pressure changes will recover by flow to the water table on a time scale depending on the depth and vertical hydraulic diffusivity. As this flow takes place, it will apply stress to the strainmeter (e.g., relative tensional stress as fluid pressure decreases), leading to apparent recovery, or partial recovery, of the coseismic static strain step. This apparent recovery has the potential to mask the time-dependent effects of horizontal pore fluid flow or viscous relaxation that might be related to tectonic post-earthquake processes. For example, the long-term effect of post-seismic poroelastic relaxation should be to increase strain because the bulk modulus in the drained limit will be lower than the undrained bulk modulus at the time of the initial coseismic step.

To illustrate how fluid pressures change in response to coseismic strain, we use the example of the 1999 Hector Mine, California, earthquake (for which, unfortunately, there is no near-field borehole strainmeter data). The Hector Mine earthquake imposed about 30 microstrain extension on wells in the Surprise Spring basin, which is used as a

groundwater source for the Marine Corps base at 29 Palms (Figure 11). Notice that in Figure 11, some of the wells in the basin exhibited large water-level drops, while in other nearby wells there was no apparent change.

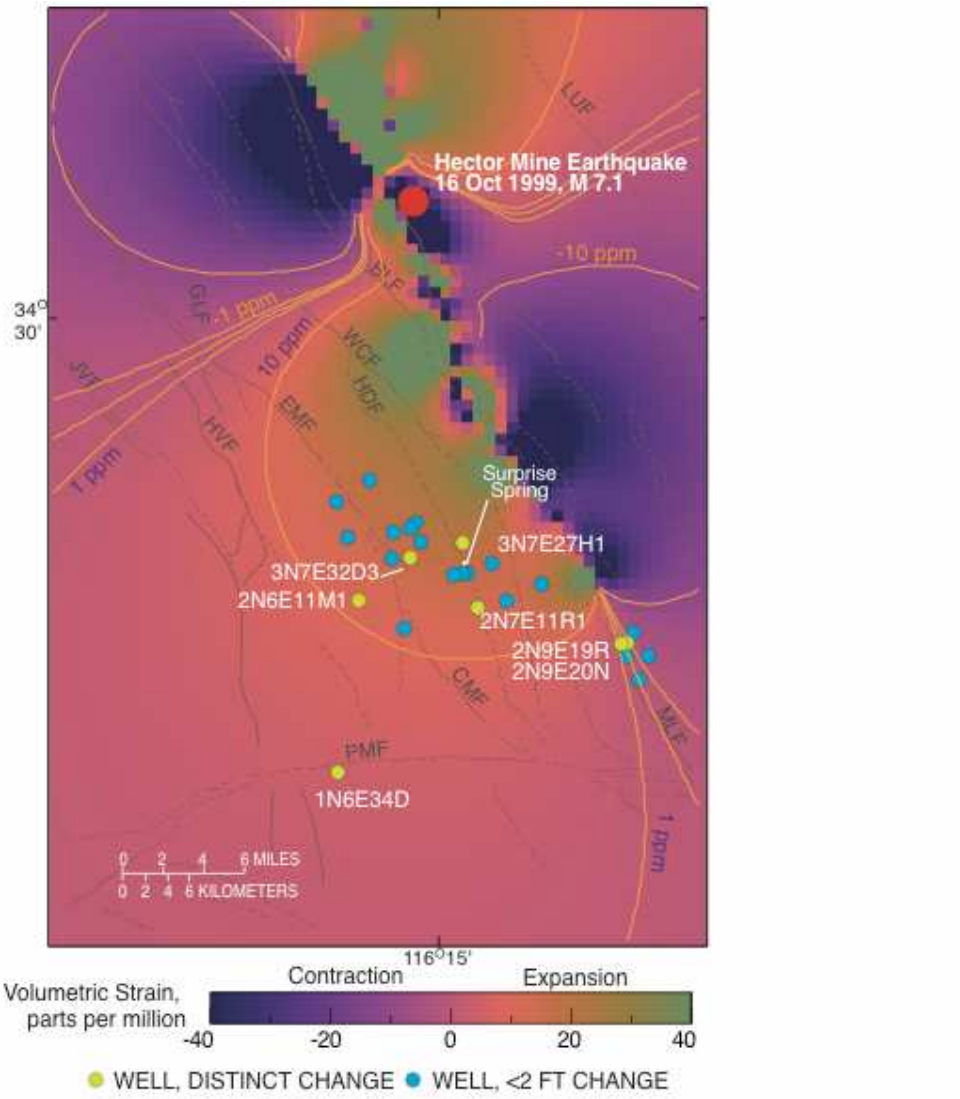

Figure 11. Calculated coseismic volumetric strain field of the M7.1 Hector Mine earthquake (October 16, 1999)

Initially, the pattern of affected and unaffected wells seemed random, but further investigation revealed that the wells that exhibited water-level drops were the deepest ones. Water levels had not been measured immediately before the earthquake, and the first post-earthquake measurements were 3 days after the earthquake. Evaluation of equation (4) for plausible diffusivities and for the depths of the wells below the water

table indicates that, in the shallower wells, the coseismic changes probably recovered within the 3 days before measurements were made (Figure 12). Note that it's important to use the depth below the water table, rather than the depth below the surface, because the water table in this area is about 100 m deep.

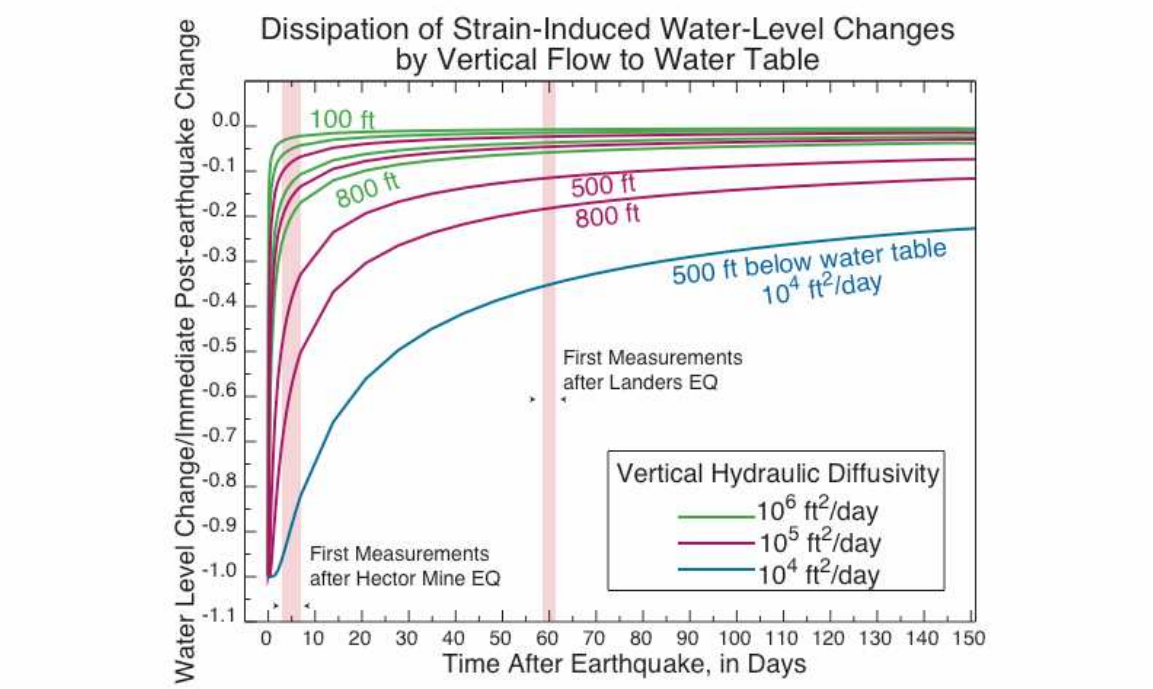

Figure 12. Hypothetical water-level time histories for wells of various depths in the Surprise Spring basin.

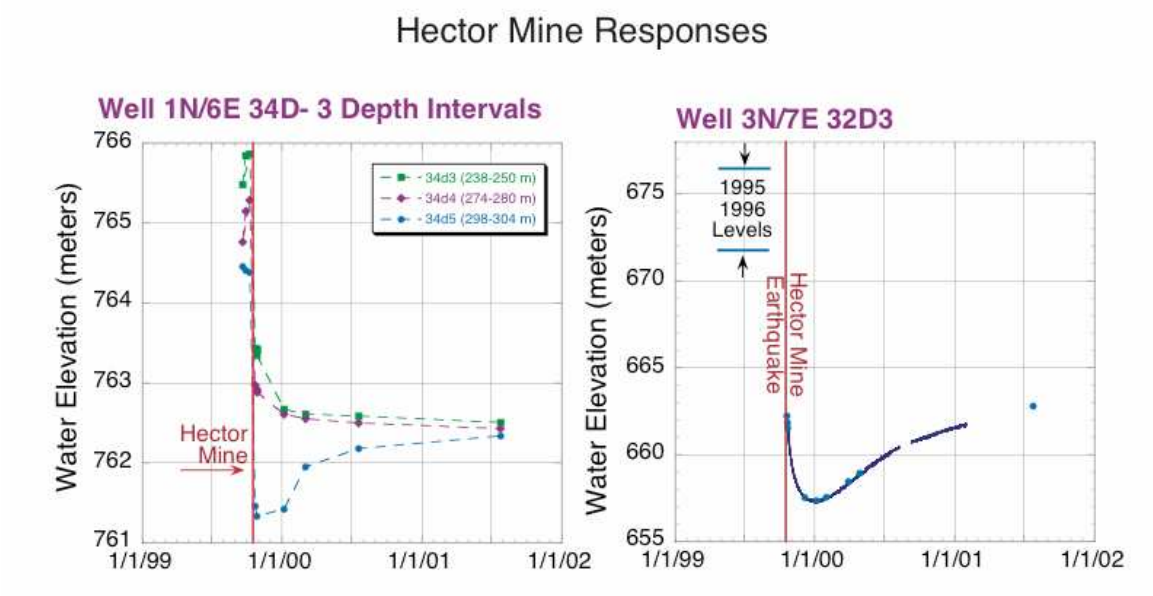

Figure 13. Water-level records from deep wells near the Hector Mine earthquake.

Figure 13 shows water-level records from wells that did experience water level drops, for a period of about a year and a half after the Hector Mine earthquake. Well 1N/6E 34D3 is monitored at three depths, and in the deepest interval the water level continued to drop for at least a couple of weeks following the earthquake; in well 3N/7E 32D3, the water level dropped an additional 5 m in the 2.5 months after the earthquake.

The mechanism causing the fluid pressure to continue to drop following the earthquake is not clear. Postseismic slip for this earthquake did not last that long, and would have been expected to affect all the levels of 1N/6E 34D3, for example. Equilibration with zones that experienced locally greater pressure drops is another possible explanation.

The mechanism for the fluid pressure recovery is almost certainly dominated by vertical flow to the water table. Horizontal flow between areas of elevated and lowered coseismic pressure change may also take place, but the distances are greater and therefore the gradients to drive flow are smaller.

The implication for a strainmeter in this area is that significant apparent strain would have been produced by these fluid-pressure changes. For example, using the approximate range of 0.02 to 1 microstrain/m of water from Table 1, apparent strain of

0.1 to 5 microstrain could have been caused by the continuing 5 m of water-level drop at well 3N/7E 32D3.

4.3 Possible apparent strain from anomalous post-earthquake fluid pressure changes

It is now recognized that seismic waves from earthquakes can produce long-lived fluid pressure changes in areas too far from the hypocenter to experience significant static strain. Presumably, these fluid-pressure changes can induce borehole strain signals. An example where this may be happening is the Postpile dilatometer at Long Valley caldera. This dilatometer recorded a week-long contractional transient beginning at the time of the 1992 M7.3 Landers earthquake over 400 km away (Hill et al, 1995; Johnston et al. 1995; Figure 14). However, it is also known that wells in the Long Valley caldera also typically exhibit fluid-pressure changes initiated by distant earthquakes (Roeloffs et al., 2003), with some of the wells typically having pressure increases, and others having drops. Furthermore, we saw above that the Postpile dilatometer has a large seasonal signal consistent with a high coefficient between apparent contractional strain and fluid pressure increase.

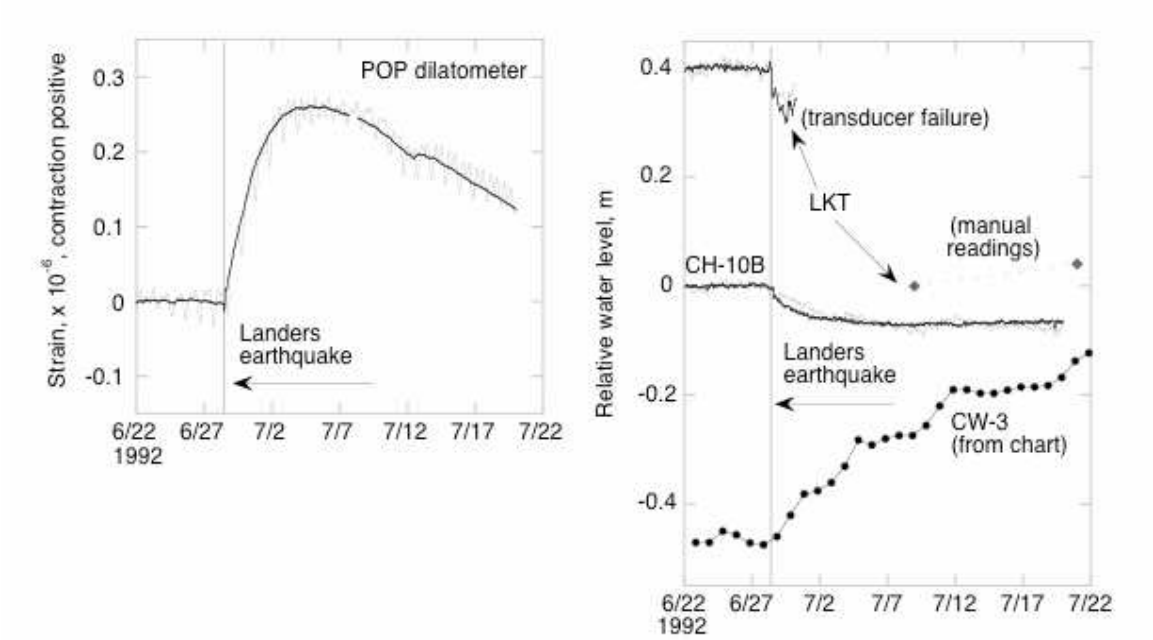

Figure 14. Dilatometer and water-level data from Long Valley caldera around the time of the 1992 Landers earthquake. The monitoring wells shown are within the caldera, 15-20 km east of the dilatometer. From Roeloffs et al. (2003).

For this reason, it seems possible that the contractional strain transient could have been caused by a fluid pressure increase at the Postpile site. Unfortunately, there has not been another induced postseismic contractional strain transient at Postpile since installation of the nearby monitoring well.

4.4 Drainage effects on strainmeter response

Dissipation of strain-induced fluid pressure by flow to the water table was introduced in section 4.1 from the viewpoint of an instantaneously imposed strain step. The length of time that the strain-induced pressure step will last depends on the depth below the water table and on the vertical hydraulic diffusivity of the overlying formation. Now we consider the same idea, but in the frequency domain. The fact that time is required for flow to the water table means that rapid fluid pressure oscillations are less susceptible to drainage effects than slow variations. At the frequency, ω, such that

$\omega(z-z_w)^2/c = 0.2$, drainage reduces the amplitude of the pressure oscillation by a factor of 1/*e* times the undrained response. Periods much shorter than this are not affected by drainage, but longer periods will be increasingly affected. Figure 10 can also be used to visualize this period as a function of depth and diffusivity. Comparing Figures 9 and 10 shows that for vertical diffusivities at the upper end of the expected range for fractured igneous rocks, drainage at a depth of 200 m may influence signals with periods of days.

When a strainmeter is subjected to strain at a period long enough for drainage to occur, its apparent sensitivity to strain will be lower than at undrained periods. An undrained contractional strain is accompanied by elevated fluid pressure that acts to further compress the strainmeter. When drainage occurs, this elevated fluid pressure is not there, so the strainmeter experiences less compression, even though the strain of the rock is the same. Under these conditions, the strainmeter will have a frequency response whose gain drops with increasing period. We saw in an earlier chapter that the frequency response of a dilatometer can be estimated by calculating its cross-spectrum with atmospheric pressure, and that at least two California dilatometers (Vineyard Canyon and Sunol) have frequency response that decreases at periods of days.

Jonsson et al. (2003) have raised the possibility that a borehole strainmeter could be installed in a location that is essentially decoupled from crustal strain on a scale of more than a few meters from the borehole. This situation requires not only that drainage occur at periods of days or less, but also that almost all strain be accommodated by deformation of pore space or fractures. The concern is motivated by the behavior of the BUR dilatometer in Iceland, for which the responses to two different earthquakes and two different volcanic eruptions have been essentially the same, after scaling by the maximum magnitude, and consist of a rapid step followed by a decay over 3-4 days. The long-term record of data from this instrument shows negligible long-term strain. A preliminary analysis of the atmospheric pressure response of the instrument shows that its response to atmospheric pressure fluctuations falls off at long periods, with a noticeable effect at periods of several days.

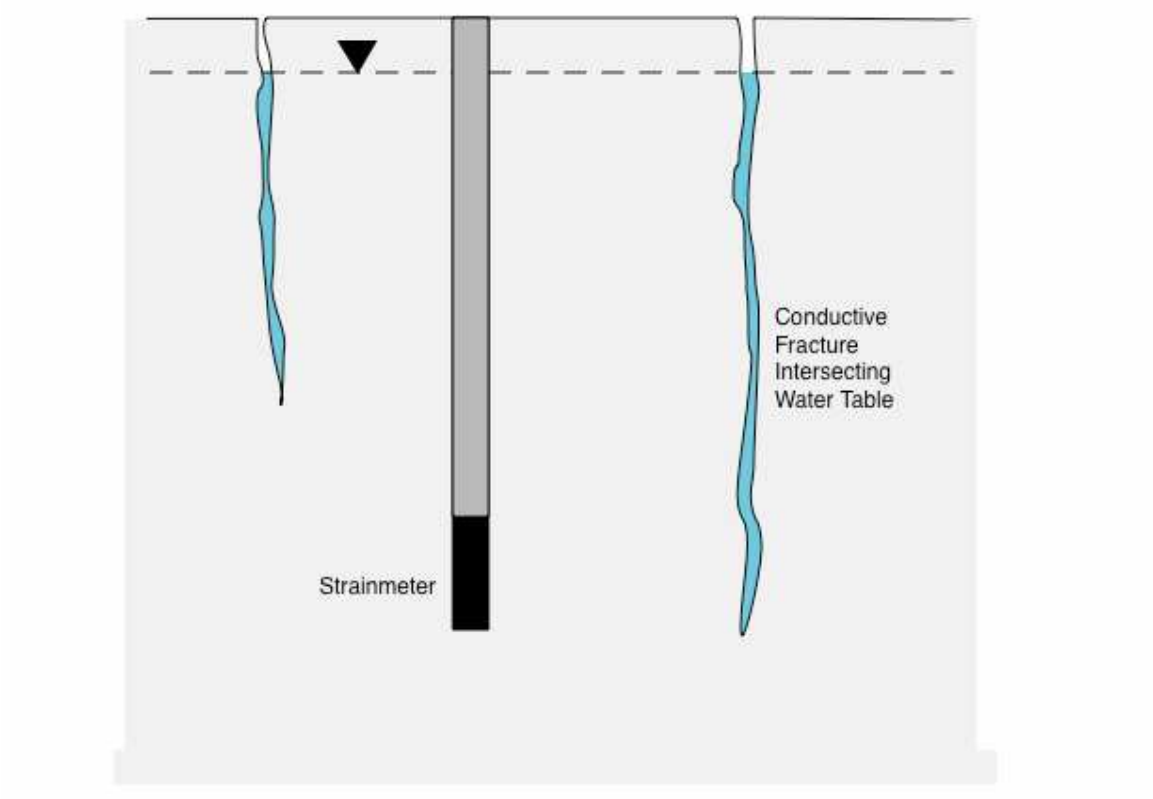

Figure 15. Cartoon showing a situation in which a strainmeter could be decoupled from regional strain.

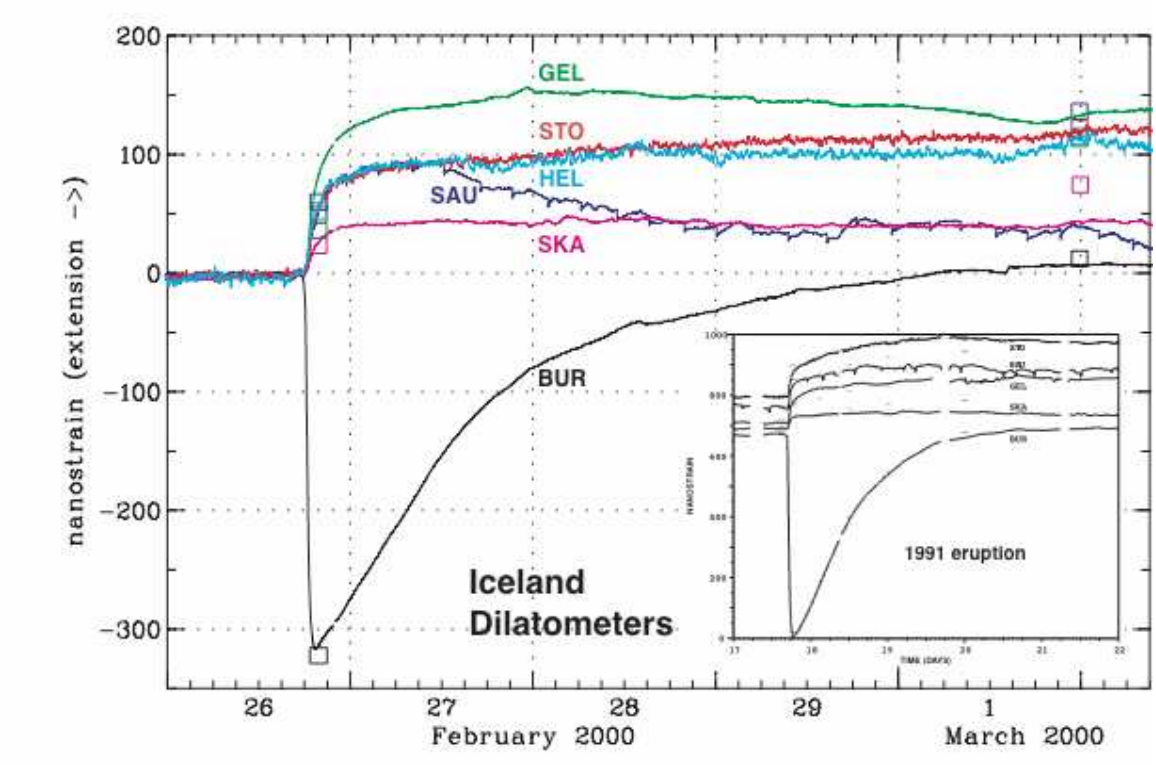

Figure 16. Data from Iceland strainmeters for two eruptions of Hekla volcano. From Roeloffs and Linde (2005).

Evidence of this type of behavior was sought in the California borehole strain data set. The features sought were: lack of long-term strain accumulation; coseismic steps that recover after short periods of time; lack of response to long-period atmospheric pressure changes; and significant differences in tidal phase from those predicted. A number of sites exhibit one of these features but in most cases can be shown not to demonstrate other features indicative of decoupling. Only the Phillips dilatometer at Long Valley, which has long been acknowledged as a poorly performing instrument, was judged possibly decoupled to the same extent as BUR.

References cited

Biot, M.A., General theory of three-dimensional consolidation, Jour. Appl. Phys., 12, 155-164, 1941.

Biot, M.A., General solutions of the equations of elasticity and consolidation for a porous material, Jour. Appl. Mech., 91-96, 1956.

Bower, D.R., Bedrock fracture parameters from the interpretation of well tides, J. Geophys. Res., 88 (B6), 5025-5035, 1983.

Hill, D.P., M.J.S. Johnston, J.O. Langbein, and R. Bilham, Response of Long Valley Caldera to the Mw 7.3 Landers, California, earthquake, Journal of Geophysical Research, 100 (B7), 12,985-13,005, 1995.

Johnston, M.J.S., D.P. Hill, A.T. Linde, J. Langbein, and R. Bilham, Transient deformation during triggered seismicity from the 28 June 1992 Mw=7.3 Landers earthquake at Long Valley Volcanic Caldera, California, Bull. Seismol. Soc. Am., 85 (3), 787-795, 1995.

Jonsson S, Segall P, Agustsson K, Agnew D. Local fluid flow and borehole strain in the South Iceland Seismic Zone. Eos Trans. AGU, 84 (46), Fall Meet. Suppl., Abstract G31B-0717, 2003

Lockner, D.A., S.A. Stanchits, Undrained poroelastic response of sandstones to a deviatoric stress change, *J. Geophys. Res.*, *107* (B12), 2353 doi:10.1029/2001JB001460, 2002.

Moench, A.F., Transient flow to a large-diameter well in an aquifer with storative semi-confining layers, Water Resour. Res., 21, 1121-1131, 1985.

Roeloffs, E.A., Poroelastic techniques in the study of earthquake-related hydrologic phenomena, Advances in Geophysics, 37, 135-195, 1996.

Roeloffs, E., M. Sneed, D.L. Galloway, M.L. Sorey, C.D. Farrar, J.F. Howle, J. Hughes, Water level changes induced by local and distant earthquakes at Long Valley caldera, California, J. Volc. Geotherm. Res., 127, 269-303, 2003.

Roeloffs E, Linde AT. Borehole observations of continuous strain and fluid pressure. In Volcano Geodesy, D. Dzurisin, in press, 2005.

Segall, P., S. Jónsson, K. Agustsson, When is the strain in the meter the same as the strain in the rock?, *Geophys. Res. Letters,* v. 30, no 19, doi:10.1029/2003GL017995, 2003.

Wang, H.F., Theory of linear poroelasticity with applications to geomechanics and hydrogeology, 287 pp., Princeton University Press, 2000.

Woodcock, D., and E. Roeloffs, Seismically-induced water level oscillations in a fractured-rock aquifer well near Grants Pass, Oregon, Oregon Geology, 58 (2), 27-33, 1996.

Online Resource

California Data Exchange Center

-snowpack, rainfall, temperature, and streamflow data for California

http://cdec.water.ca.gov/